



HAL
open science

Estimating Drill String Friction Parameters: Comparing Performance of Model-Based Estimators to a Data-Driven Neural Network

Jean Auriol, Roman Shor, Silviu-Iulian Niculescu, Nasser Kazemi

► **To cite this version:**

Jean Auriol, Roman Shor, Silviu-Iulian Niculescu, Nasser Kazemi. Estimating Drill String Friction Parameters: Comparing Performance of Model-Based Estimators to a Data-Driven Neural Network. 2021. hal-03250640

HAL Id: hal-03250640

<https://hal.science/hal-03250640>

Preprint submitted on 4 Jun 2021

HAL is a multi-disciplinary open access archive for the deposit and dissemination of scientific research documents, whether they are published or not. The documents may come from teaching and research institutions in France or abroad, or from public or private research centers.

L'archive ouverte pluridisciplinaire **HAL**, est destinée au dépôt et à la diffusion de documents scientifiques de niveau recherche, publiés ou non, émanant des établissements d'enseignement et de recherche français ou étrangers, des laboratoires publics ou privés.

Estimating Drill String Friction Parameters: Comparing Performance of Model-Based Estimators to a Data-Driven Neural Network

Jean Auriol¹, Roman Shor², Silviu-Iulian Niculescu¹ and Nasser Kazemi²

Abstract—In this paper, we consider the torsional motion of a drilling system and propose three algorithms to estimate the friction factors that characterize the interaction between the drill pipe and the wellbore walls (Coulomb source terms). This is essential to design the next generation of stick-slip mitigation controllers, to develop real-time wellbore monitoring tools, and to enable effective toolface control for directional drilling. We propose two model-based algorithms (an adaptive observer and a recursive dynamics framework) and a machine learning-based algorithm to estimate friction parameters, all of them presenting advantages and drawbacks. The performances of our model-based estimators are finally compared with this data-driven neural network.

I. INTRODUCTION

Extraction of resources in the earth’s subsurface - oil, gas, minerals, and thermal energy - necessitates the drilling of long slender boreholes from the surface to the subsurface target. The diameters of these wells range from 10 to 50 cm, and lengths can frequently exceed 10,000 m, leading to mechanical systems with extreme aspect ratios. These drill strings consist of sections of steel drill pipe and stiffer drill collars. Transfer of energy (rotational and axial) often leads to complex dynamic behaviors, which often manifest themselves as drill string vibrations and has been extensively studied [5], [16] or [24] for a more complete review.

A particular vibration pattern that is prevalent is called stick-slip, where self-excited torsional oscillations manifest themselves in the drill string and are caused by friction along the wellbore between the drill pipe and the wellbore wall and by the bit-rock interaction. These stick-slip oscillations are generally characterized by a series of stopping – “sticking” – and releasing – “slipping” – events of the bit.

This phenomenon has been studied extensively and has been explained through a non-linear, or velocity-weakening - effect of bit-rock interaction [10], [18], through distributed friction between the drill pipe and the wellbore wall [1] or through a combination of both [7], [16], [23]. This is of particular importance in modern wellbores, which are rarely straight and must follow pre-planned well plans, ranging from simpler horizontal or deviated wells to complex three-dimensional paths, thus increasing the effect of torque and drag.

During directional drilling operations, downhole measurements are usually available. They are obtained by combining accelerometers or gyroscopes and one to three-axis magnetometers. These sensors are sampled at frequencies between 1-100 Hertz by the downhole tool but only averaged or windowed values are transmitted to surface [12]. Thus, these measurements are transmitted to the surface

infrequently (once per minute to once per hour) and with a significant delay (on the order of seconds). Although this is not a problem for human-in-the-loop operations, it becomes insufficient for automated solutions. Such delays and sampled measurements imply significant performance degradation when using feedback controllers that aim to compensate stick-slip oscillations [3]. Real-time estimation of friction parameters [13] enable feedforward [4] control as well as a new generation of controllers based on the backstepping methodology [14] and thereby allow better performance.

In the present work, we propose three strategies (two of them being completely original) to estimate these Coulomb friction factors. Two of them are model-based (adaptive observer and recursive dynamics framework), while the last one is based on machine-learning. The model we use for the two first approaches is adjusted from [1]: the bit is off-bottom (we do not consider bit-rock interaction), and Coulomb friction is included as a source term implemented as an inclusion.

This paper is structured as follows: it begins with a brief derivation of the drill string model in section II, followed by the description of three methods to estimate friction:

- 1) Section III describes the adaptive observer,
- 2) Section IV describes the recursive dynamics framework, and
- 3) Section V describes the machine learning approach

Finally, in Section VI the three approaches are compared with data generated by the model described in section II.

II. MODEL UNDER CONSIDERATION

In this section, we present the mathematical model developed in [1] to describe the torsional dynamics of the drill string. The proposed model is relatively simple (which makes it usable for control and estimation perspectives) and realistic since it has been validated against field data. The main assumptions we use are the following:

- The torsional motion of the drill string is the dominating dynamic behavior.
- Uniform axial motion. No distributed axial dynamics.
- We consider that the bit is off-bottom, i.e., there is no bit-rock interaction.
- The transition from static to dynamic Coulomb friction is modeled as a jump, i.e., the Stribeck curve is assumed negligible.
- The effects of along-string cuttings distribution on the friction is assumed to be homogeneous.
- The effect of the pressure differential, inside and outside the drill string, on the bending moment, is considered to be negligible.

¹Jean Auriol, and Silviu-Iulian Niculescu are with Université Paris-Saclay, CNRS, CentraleSupélec, Inria, Laboratoire des Signaux et Systèmes, 91190, Gif-sur-Yvette, France. ²Roman Shor and Nasser Kazemi are with the University of Calgary, Calgary, Alberta, Canada. Corresponding author: jean.auriol@centralesupelec.fr

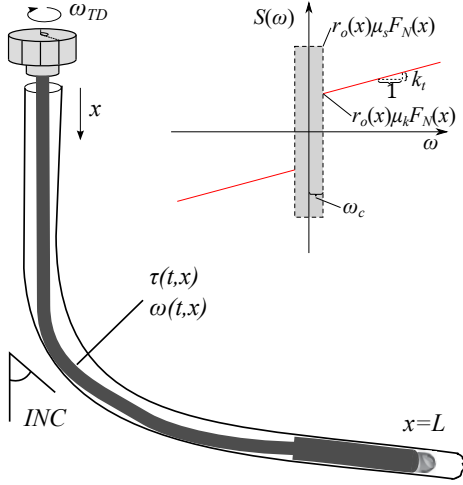


Fig. 1. Schematic indicating the distributed drill string of length L lying in deviate borehole. Inset: Schematic illustrating the friction source term $S(\omega, x)$. The shaded region represents the angular velocities for which a constant value of static torque is assumed and the red curve indicates the dynamic torque as a function of angular velocity.

A. Torsional dynamics of the drill string

We consider that the torsional motion of the drilling device corresponds to the dominating dynamic behavior. The distributed model we present here is adjusted from [1] (where the reader can find the complete model derivation). This kind of representation is popular in the literature [5], [16]. We give a schematic representation of the drill string in Fig. 1. Let us denote the angular velocity and torque as $\omega(t, x)$, $\tau(t, x)$, respectively, with $(t, x) \in [0, \infty) \times [0, L]$ (L being the length of the drill string). We have

$$\frac{\partial \tau(t, x)}{\partial t} + JG \frac{\partial \omega(t, x)}{\partial x} = 0 \quad (1)$$

$$J\rho \frac{\partial \omega(t, x)}{\partial t} + \frac{\partial \tau(t, x)}{\partial x} = S(t, x), \quad (2)$$

where, J is the polar moment of inertia, G the shear modulus and ρ the drill string density. The source term S is given as

$$S(t, x) = -k_t \rho J \omega(t, x) - \mathcal{F}(t, x), \quad (3)$$

where the damping constant k_t is the viscous shear stresses and where \mathcal{F} is a differential inclusion that corresponds to the Coulomb friction between the drill string and the borehole, also known as the side force. We use the following inclusion to implement the side force

$$\begin{cases} \mathcal{F}(t, x) = r_o(x) \mu_k F_N(x), & \omega(t, x) > \omega_c, \\ \mathcal{F}(t, x) \in \pm r_o(x) \mu_s F_N(x), & |\omega(t, x)| < \omega_c, \\ \mathcal{F}(t, x) = -r_o(x) \mu_k F_N(x), & \omega(t, x) < -\omega_c, \end{cases} \quad (4)$$

where μ_s is the static friction coefficient (i.e. the friction between two or more solid objects that are not moving relative to each other) and μ_k is the kinetic friction coefficient (also known as dynamic friction or sliding friction, which occurs when two objects are moving relative to each other and rub together), ω_c is the threshold on the torsional velocity where the Coulomb friction transits from static to dynamic. The function F_N is the normal force acting between the drill string and the borehole wall. The function $\mathcal{F}(\omega) \in$

$\pm r_o(x) \mu_s F_N(x)$ denotes the inclusion where

$$\begin{aligned} \mathcal{F}(t, x) &= -\frac{\partial \tau(t, x)}{\partial x} - k_t \rho J \omega(t, x) \\ &\in [-r_o(x) \mu_s F_N(x), r_o(x) \mu_s F_N(x)], \end{aligned} \quad (5)$$

and take the boundary values $\pm \mu_s F_N(x)$ if this relation does not hold. The shape of the friction source term is illustrated in Fig. 1.

The method to calculate normal force, to account for discontinuities of a multiple sectioned drill string and the Riemann invariants may be found in [1].

B. Boundary condition

We consider that the drilling device is actuated at the top-drive by a motor torque: τ_m . To reach a given reference velocity set-point ω_{SP} , we consider a standard PI control law [6]:

$$\tau_m = k_p(\omega_{SP} - \omega_0) + k_i \int_0^t (\omega_{SP}(\xi) - \omega_0(\xi)) d\xi, \quad (6)$$

where k_p is a proportional gain and k_i an integral gain. We denote J_{TD} the topdrive inertia and where ω_0 verifies the following equation

$$\frac{\partial \omega_0}{\partial t} = \frac{1}{J_{TD}} (\tau_m - \tau(t, 0)). \quad (7)$$

Finally, since the bit is off-bottom, we have $\tau(t, L) = 0$.

C. Estimation problem

As detailed in the introduction, the design of the next generation of stick-slip mitigation controllers requires reliable estimations of the friction parameters. In the rest of the paper, we present three methods to estimate all (or part) of the friction parameters. We emphasize their advantages and their drawbacks. Data measurements correspond to the top-drive torque and velocity.

III. FIRST APPROACH: ADAPTIVE OBSERVER

The first approach we propose is adjusted from the adaptive state-observer proposed in [2]. Although the results given in [2] correspond to the case of a two-sections drilling device (i.e., the drill string is made of only two sections: the pipe and the collar), they can be extended to the case of a multi-sectional drill string, either by adjusting the theoretical approach given [14] or the new recursive framework proposed in [22]. This observer combines measurements from physical sensors (top-drive angular velocity ω_0) with the proposed model of the system dynamics. It provides reliable estimates of the torque and RPM states and of the side forces friction parameters when the bit is off bottom [2]. We recall here the main ideas of this observer.

Let us denote with the $\hat{\cdot}$ superscript the estimated states and $e = \hat{\omega}_0 - \omega_0$ the measured estimation error of the top-drive angular velocity. The observer equations given in [2] in terms of Riemann invariants read as follows (the index i corresponds to the considered section of the drill-string)

$$\dot{\hat{\omega}}_0 = a_0 \left(\hat{\beta}_p(t, 0) - \hat{\omega}_0 \right) + \frac{1}{I_{TD}} \tau_m - p_0 e, \quad (8)$$

$$\frac{\partial \hat{\alpha}^i}{\partial t}(t, x) + (c_t)_i \frac{\partial \hat{\alpha}^i}{\partial x}(t, x) = \hat{S}^i(t, x) - p_\alpha^i(x) e, \quad (9)$$

TABLE I
ADVANTAGES AND DRAWBACKS OF ALGORITHM 1

Advantages	Drawbacks
Correct estimations μ_s, μ_k , when testing in simulations and against field data [2].	Requires the knowledge of ω_c
Convergence guaranteed in the absence of friction terms [14]	No proof of convergence for the adaptive part
Real-time estimation robust to uncertainties and delays	Persistent excitation for the adaptive part

$$\frac{\partial \hat{\beta}^i}{\partial t}(t, x) - (c_t)^i \frac{\partial \hat{\beta}^i}{\partial x}(t, x) = \hat{S}^i(t, x) - p_\beta^i(x)e, \quad (10)$$

The source term in each section is computed from the estimated states and friction factor:

$$\hat{S}^i(t, x) = k_t(\hat{\alpha}^i(t, x) + \hat{\beta}^i(t, x)) + \frac{1}{J^i \rho^i} \hat{F}^i(t, x), \quad (11)$$

where \hat{F} has an expression identical to (4), the different variables being replaced by their estimates. The different boundary conditions now express as

$$\hat{\alpha}(t, 0) = 2\hat{\omega}_0(t) - \hat{\beta}(t, 0) - P_0 e, \quad (12)$$

$$\hat{\beta}^i(t, x_{i+1}) = \frac{\hat{\alpha}^i(t, x_{i+1})(1 - \bar{Z}^i) + 2\bar{Z}^i \hat{\beta}^{i+1}(t, x_{i+1})}{1 + \bar{Z}^i} - P_1 e, \quad (13)$$

$$\hat{\alpha}^{i+1}(t, x_{i+1}) = \frac{2\bar{Z}^i \hat{\alpha}^i(t, x_{i+1}) - \hat{\beta}^{i+1}(t, x_{i+1})(1 - \bar{Z}^i)}{1 + \bar{Z}^i}, \quad (14)$$

$$\hat{\beta}(t, L) = \hat{\alpha}(t, L), \quad (15)$$

and the estimates of the friction factor are updated according to

$$\hat{\mu}_s(t) = \begin{cases} -l_s e, & |\min_x \hat{\omega}(t, x)| \leq \omega_c, \\ 0, & |\min_x \hat{\omega}(t, x)| > \omega_c, \end{cases} \quad (16)$$

$$\hat{\mu}_k(t) = \begin{cases} 0, & |\min_x \hat{\omega}(t, x)| \leq \omega_c, \\ l_k e, & |\min_x \hat{\omega}(t, x)| > \omega_c, \end{cases} \quad (17)$$

Finally, we use a saturation to improve the robustness of the approach: $\hat{\mu}_s = \max(\hat{\mu}_s, \hat{\mu}_k)$. The different constants and observer gains $a_0, p_\alpha^i, p_\beta^i, p_0, p_1, P_0, P_1, l_s, l_k$ can be found in [2]. The estimation procedure is summarized by Algorithm 1

Algorithm 1 Estimation of μ_k and μ_k with an adaptive observer.

Require: $\tau_m, \omega_0, \omega_c$

- 1: Simulate system (8)-(15) with the adaptive laws (16)-(17)
- 2: $\hat{\mu}_s = \max(\hat{\mu}_s, \hat{\mu}_k)$.

Output

$$\hat{\mu}_k \leftarrow \lim_{\infty} \hat{\mu}_k(t) \quad \hat{\mu}_s \leftarrow \lim_{\infty} \hat{\mu}_s(t).$$

The advantages and drawbacks of this adaptive observer are summarized in Table I.

IV. SECOND APPROACH: RECURSIVE DYNAMICS FRAMEWORK

The second approach we propose corresponds to a *recursive dynamics interconnection framework*. Such a framework is particularly suited for sensing and estimation since it

allows structuring the model on some simpler and more realistic interconnected dynamical subsystems (blocks) and better exploiting the interconnection structure. The method has been developed in [8] to estimate the nature of the rock interacting with the drill string (only the axial motion was considered). We believe it can be extended to torsional oscillations to estimate the friction parameters. Let us mention that if all the points of the drill string reach the kinematic mode, then the function $\mathcal{F}(t, x)$, defined by (4), does not (directly) depend on time anymore. Thus, similar to what has been done in [8], it becomes possible to apply successive backstepping transformations to each section of the drill string to simplify the structure of each block. Denote by x_i the spatial coordinate of the junction point between two sections of the drill string. Using the method of characteristics and the continuity of torque and velocity, we can express the state at $x = x_i$ as a function of delayed and future state values at $x = x_{i+1}$. More precisely, we have

$$\omega^i(t, x_{i+1}) = f^i(\omega^i(\cdot, x_i), \tau^i(\cdot, x_i)) + h_\omega^i \quad (18)$$

$$\tau^i(t, x_{i+1}) = g^i(\omega^i(\cdot, x_i), \tau^i(\cdot, x_i)) + h_\tau^i, \quad (19)$$

where f^i and g^i are two functions that only depend on the physical parameters of the drilling device (except μ_k) and past and future values of $\omega^i(\cdot, x_i)$ and $\tau^i(\cdot, x_i)$, the largest time-shift being fixed by the parameters of the system. The functions h_ω^i and h_τ^i are constant functions that linearly depend on μ_k . Computations to obtain explicit expressions for these different functions are quite involved and cannot be given here due to space restrictions. They follow the same path as the ones given in [8]. Using equations (18) and (19), we can express $\tau(t, L)$ as a function of top-drive angular velocity and torque measurements. Since the bit is off-bottom, we know that $\tau(t, L) = 0$. Thus, it becomes possible to use classical regression techniques (such as Recursive Least Squares) to estimate the kinematic coefficient μ_k . Indeed, if we have M measurement points, this coefficient is estimated by minimizing the following cost function

$$\{\hat{\mu}_{kin}\} = \underset{\mu_k}{\operatorname{argmin}} \sum_{i=1}^M (\hat{\tau}(t_i, L))^2, \quad (20)$$

where $\hat{\tau}(t_i, L)$ is the estimated version of the torque obtained using equations (18) and (19). Obviously, the proposed estimation of the torque-on-bit only holds if we have $\omega > \omega_c$ all over the drill string (otherwise, non-linear terms appear, which makes the estimation extremely difficult). Thus, we need to apply equations (18) and (19) to all points of the drill string (in practice, to a sufficiently large number of points) to verify that it is the case. Among all the estimations of the drill-bit source signature, only the ones for which this condition is fulfilled can be used to estimate the kinematic friction term. Note that this estimation procedure is done in near real-time (contrary to the previous adaptive observer which is done in real-time) due to the fact that (18) and (19) require future values of the measurements.

To verify that the condition $\omega > \omega_c$ is satisfied, we need the knowledge of ω_c . However, knowing a decent upper-bound could be sufficient and provide an estimation of ω_c . More precisely, let us denote $\bar{\omega}_c$ such an upper-bound. Applying the previous procedure for $\omega > \bar{\omega}_c$ all over the drill string, we can estimate μ_k , assuming that enough data points

TABLE II
ADVANTAGES AND DRAWBACKS OF ALGORITHM 2

Advantages	Drawbacks
Reliable estimation of μ_k	Near-real time algorithm
Procedure to estimate ω_c	μ_s is not estimated
Good robustness properties [8]	Computationally expensive ($\hat{\tau}^i$)

verify these conditions (to apply the least-squares algorithm). Note that we can modify the reference set-point in the PI control law to guarantee this last condition. Then, since μ_k is now known, we can reiterate the estimation procedure while decreasing the bound $\bar{\omega}_c$. Once the quadratic error $\sum_{i=1}^M (\hat{\tau}(t_i, L))^2$ becomes larger than a chosen threshold ϵ , it means that we have reached ω_c since the non-linear static friction terms are now modifying our estimation of the torque on the bit. This procedure is described by Algorithm 2. The values of ω_c are updated using a dichotomy approach (tolerance η). The threshold ϵ should be large enough to encompass measurement noise. The advantages and drawbacks of this estimation procedure are summarized in Table II.

Algorithm 2 Estimation of μ_k and ω_c with a recursive dynamics framework.

Require: $\tau(t, 0)$, $\omega(t, 0)$, $\bar{\omega}_c$, $\underline{\omega}_c$, ϵ , η

- 1: Compute $\hat{\tau}_i(t, L)$ with equations (18) and (19) for all the data points that verify $\hat{\omega}(t, x) > \bar{\omega}_c$, for all t .
- 2: Recursive Least Squares algorithm: $\{\hat{\mu}_{kin}\} = \underset{\mu_k}{\operatorname{argmin}} \sum_{i=1}^M (\hat{\tau}(t_i, L))^2$.
- 3: Update $\omega_c^k: \frac{\underline{\omega}_c + \bar{\omega}_c}{2}$
- 4: Compute $S = \sum_{i=1}^M (\hat{\tau}(t_i, L))^2$ for all the data points that verify $\hat{\omega}(t, x) > \omega_c^k$.
- 5: If $S > \epsilon$, $\underline{\omega}_c \leftarrow \omega_c^k$. Else, $\bar{\omega}_c \leftarrow \omega_c^k$.
- 6: If $\bar{\omega}_c - \underline{\omega}_c > \eta$ go to Step 3.

Output

$$\hat{\mu}_k \leftarrow \hat{\mu}_k, \quad \hat{\omega}_c \leftarrow \omega_c^k.$$

V. THIRD APPROACH: MACHINE LEARNING ESTIMATION

The third approach we present in this paper is based on Machine Learning ([17]). Hence, it does not require any specific knowledge of the system or an accurate model. Note that adaptive neural networks have already been applied in [15] or [28] for control purposes. The main idea behind this approach is that the measured top-drive torque and angular velocity (or in closed-loop the output of the PI control law) depend on the geometry and the physical parameters of the drilling device (and in particular of the friction factors). Thus, the spectrum of these signals should contain sufficient information to estimate the static and kinematic friction terms. Let us denote $y(t) = \tau_m(t)$ the measured motor torque (that is related to ω_0 due to (6)). Due to the top-drive sensors sampling rate, this signal is not updated continuously. We will denote Y the vector obtained by concatenating the different values of y at each sampling step. We then compute the discrete Fourier transform of Y to obtain the spectrum of the signal y . We recall that the discrete Fourier transform of a signal Y with M components is a complex function that

is defined by

$$\hat{Y}(k) = \sum_{n=1}^M y(k) e^{-2\pi i k \frac{(k-1)(n-1)}{M}}. \quad (21)$$

The spectrum of the signal y is characterized by several *attributes*: the number of peaks, the dominant peak (highest value of the modulus of \hat{Y}), the dominant peak after a given cut-off frequency, the corresponding frequencies. The values of some of these attributes are related to the physical parameter of the systems. Thus, for a set of known physical parameters that characterize the well (including its geometry), we can run thousands of simulations, only modifying the parameters we want to estimate (namely μ_k and μ_s) between each simulation. This gives us a set of data (known as *training set*) for which the correct values of the friction parameters are known. Our algorithm will learn from this data set and find the suitable correlations between the previously defined attributes and the unknown parameters. Once adequately trained, the machine can be applied to make accurate predictions for new data sets.

We choose to develop a neural network algorithm using a sigmoid activation function [17], [21]. The network is trained by simulating thousands of test points for which we know the correct values of the friction parameters. From these simulations, we generate the spectrum of the corresponding output signals and compute several relevant features. While training our neural network, it appeared that the relevant attributes for learning are the two dominant gains (and their corresponding frequencies). We then design our neural network (i.e., we choose the number of neurons, layers, weights) and train it using *cross-validation*. The algorithm is now ready to be applied to an unknown dataset. The details of the algorithm are summarized in Algorithm 3. The

Algorithm 3 Estimation of μ_s and μ_k using a ML algorithm

Require: $\tau_m(t)$, training dataset $(\tau_m^k(t), \mu_k^k, \mu_s^k)$

Training of the network

- 1: Compute the Fourier transform of $\tau_m^k(t)$ using (21)
- 2: Compute the two dominant gains and the corresponding frequencies
- 3: Using cross-validation, design a neural network with `sklearn.neural_network.MLPRegressor`

Estimation

- 4: Compute the Fourier transform of $\tau_m(t)$
- 5: Compute the two dominant gains and the corresponding frequencies
- 6: Run the neural network with this new point

Output

$$\hat{\mu}_s \leftarrow \hat{\mu}_s, \quad \hat{\mu}_k \leftarrow \hat{\mu}_k$$

advantages and drawbacks of this machine learning algorithm are summarized in Table III.

The generalizability of a convolutional neural network depends on the number of learnable free parameters and the depth of the neural network [9], [29]. In most applications, the comprehensive dataset is not available and the learned network cannot properly model the complexities of the system. To remedy this shortcoming, one needs to take advantage of active learning, model-based learning, and transfer learning to make the learned mapping function general enough so that the learned operator gives proper

TABLE III
ADVANTAGES AND DRAWBACKS OF ALGORITHM 3

Advantages	Drawbacks
Reliable, and easy to implement	Lacks generalizability
Estimation of μ_k and μ_s	Requires thousands of training points
Fast algorithm (once properly trained)	Depends on the initial condition of the system

TABLE IV
MEAN AND STANDARD DEVIATION (IN PARENTHESIS) OF THE FRICTION FACTORS ESTIMATION USING THE THREE PROPOSED ALGORITHMS FOR THE FIRST TEST CASE ($\mu_s = 0.34$ AND $\mu_k = 0.187$).

Algorithm	$\hat{\mu}_s$	$\hat{\mu}_k$
Adaptive observer	0.358 (0.02)	0.192 (0.01)
Recursive dynamics framework	N.A	0.1892 (0.03)
Machine learning algorithm	0.332 (0.023)	0.19 (0.01)

parameter estimation when applied on a new dataset [11], [27], [26], [19].

VI. SIMULATION RESULTS

We now test our three estimation algorithms against the simulation model given in [5] using the wellbore survey from [1], where the well is vertical for 300m, builds to 40 degrees inclination and holds until to a measure depth of 1250m and then builds and holds at 45 degrees for the remainder of the well.

A. Comparison of the three algorithms on two test cases

We first compare the three estimation algorithms on two test case studies. All the numerical values for the different parameters can be found in [5]. We consider a reference set-point for the top drive angular velocity of 60 RPM. In the first case study, the side forces static friction term is chosen to be equal to 0.42, while the kinematic friction term is equal to 0.29. In the second one, we have $\mu_s = 0.45$ and $\mu_k = 0.28$. In both cases, we have $\omega_c = 14$ RPM. We assume that the measured signals are subject to a white Gaussian noise that is characterized by its signal-to-noise ratio (SNR) [20]. Seventy-five simulations and estimations have been performed for each algorithm. The SNR for all the signals is equal to 10. We give in Table IV and Table V the mean and standard deviation for the estimations given by each algorithm.

Our three algorithms allow satisfying estimations of the friction parameters. The two first algorithms are model-based and consequently require a reliable model of the drill string dynamics (which is not the case of the machine learning algorithm). Although being the most accurate, the Recursive dynamics framework-based algorithm cannot (in its current form) provide an estimation of the static friction term. Finally, even if the Machine Learning algorithm

TABLE V
MEAN AND STANDARD DEVIATION (IN PARENTHESIS) OF THE FRICTION FACTORS ESTIMATION USING THE THREE PROPOSED ALGORITHMS FOR THE SECOND TEST CASE ($\mu_s = 0.45$ AND $\mu_k = 0.28$).

Algorithm	$\hat{\mu}_s$	$\hat{\mu}_k$
Adaptive observer	0.50 (0.015)	0.289 (0.01)
Recursive dynamics framework	N.A	0.287 (0.03)
Machine learning algorithm	0.463 (0.03)	0.285 (0.02)

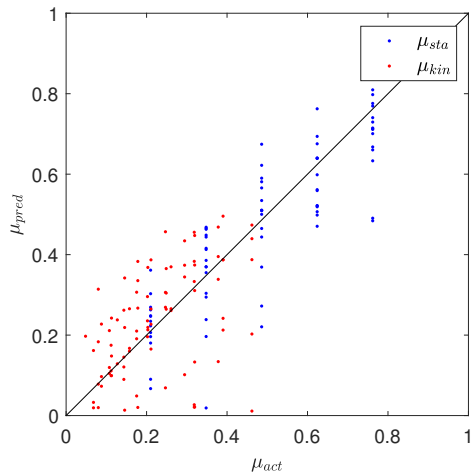


Fig. 2. Comparing real friction versus predicted friction for NN1, where the training data set has a limited range in depths. Poor performance is observed as the neural network fails to properly predict friction for depths outside of the training data set range.

shows satisfactory performance, it requires sizeable training datasets, which can be time-consuming to both generate and then subsequently train.

B. Machine Learning Results

To extend the usefulness of the data-driven model, we considered expanding the training dataset to include a range of bit depths, leading to a range in static and kinematic torques. Using two training data sets, we evaluate the performance of the neural network on a test data set generated for the considered well. Training data set 1 (DS1) contains 1000 data points with parameters ranges of $\mu_s \in [0.2, 0.83]$, $f_{rat} \in [0.2, 0.65]$ (where f_{rat} is such that $\mu_k = f_{rat}\mu_s$) and for well depths ranging from 2,500 m to 2,770 m. Training data set 2 (DS2) contains 1000 data points with the same ranges for μ_s and f_{rat} , however, well depth ranges from 1,700 m to 2,870 m. The test data set (TS) contains 125 data points with $\mu_s \in [0.210, 0.76]$, $f_{rat} \in [0.23, 0.6]$ and measure depths ranging from 1,760 m to 2,752 m. Using the algorithm described in Algorithm 3, a neural network is trained on DS1 (NN1) and on DS2 (NN2) and then applied to TS.

As the test data set contains depths outside of the range of DS1, the performance of NN1 is poor, as expected. Bit depth and the weighted average of the inclination of the drill pipe are used as additional input parameters. However, the neural network cannot generalize the predictions as no implicit knowledge of drill string dynamics is embedded in the neural network. Figure 2 shows the actual vs predicted friction values for the training data set, with static friction shown in blue and kinematic friction shown in red.

NN2 performs well when applied to the data in TS as the TS2 spans the input parameter range, for μ_s , μ_k and bit depth. It is noted that estimates of static friction are worse than the estimated of kinematic friction, as is expected. Figure 3 shows the actual vs predicted values of friction for the training data set.

This shows that the machine learning model is generalizable, so long as the training data set spans a sufficient parameter space. Future work in embedding some of the

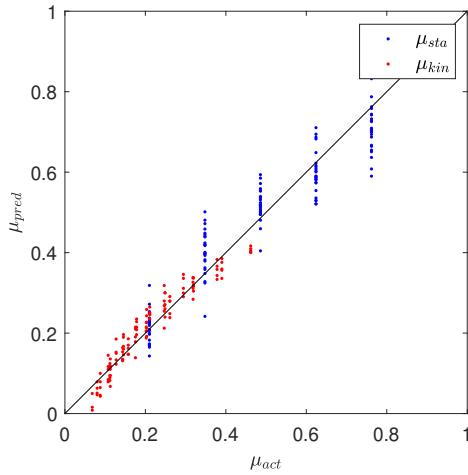


Fig. 3. Comparing real friction versus predicted friction for NN2, where the training data set includes the range of depths included in the test data set. Performance is significantly improved, particularly for kinematic friction.

basic physical properties of the drill string system into the neural network may improve performance outside of the training parameter space. Some preliminary work has been in this space for seismic data processing and inversion shows promise for application to problems governed by the wave equation [25].

VII. CONCLUDING REMARKS

In this paper, we have designed three algorithms that provide real-time or near real-time estimations of the friction factors corresponding to the side-forces acting on a drilling device. Estimating these parameters is a well-known challenge in the drilling industry and, if understood, presents the opportunity to improve drilling operations through feed-forward or model predictive control. It is a crucial step to develop stick-slip mitigation strategies. The three proposed procedures correspond to an adaptive observer (originally introduced in [2]), to an algorithm based on recursive dynamics framework, and to a machine learning algorithm. All of them only require surface measurements, making them realistically implementable on drilling devices. Their specific advantages and drawbacks have been emphasized. These algorithms have then been implemented on a previously validated torsional drill string model, with specific attention paid to the machine learning procedure. This algorithm is easy to implement and fast to run once properly trained but may not be robust to changes in the system parameters (as a new long training phase would be necessary). The three algorithms provide satisfying estimations of the friction parameters. Future works should include testing against field data and an analysis of the computational effort for each procedure. The expected outcome is a hybrid strategy to estimate friction parameters in drilling.

REFERENCES

- [1] U. J. Aarsnes and R. J. Shor. Torsional vibrations with bit off bottom: Modeling, characterization and field data validation. *Journal of Petroleum Science and Engineering*, 163:712–721, apr 2018.
- [2] U. J. F. Aarsnes, J. Auriol, F. Di Meglio, and R. J. Shor. Estimating friction factors while drilling. *Journal of Petroleum Science and Engineering*, 179:80–91, 2019.

- [3] U. J. F. Aarsnes, F. di Meglio, and R. Shor. Benchmarking of industrial stick-slip mitigation controllers. *IFAC-PapersOnLine*, 51(8):233–238, 2018.
- [4] U. J. F. Aarsnes, F. Di Meglio, and R. J. Shor. Avoiding stick slip vibrations in drilling through startup trajectory design. *Journal of Process Control*, 70:24–35, 2018.
- [5] U. J. F. Aarsnes and N. van de Wouw. Axial and torsional self-excited vibrations of a distributed drill-string. *Journal of Sound and Vibration*, 444:127–151, 2019.
- [6] K. J. Åström and R. M. Murray. *Feedback systems: an introduction for scientists and engineers*. Princeton university press, 2nd edition, 2010.
- [7] J. Auriol, U. J. F. Aarsnes, and R. Shor. Self-tuning torsional drilling model for real-time applications. In *2020 American Control Conference (ACC)*, pages 3091–3096. IEEE, 2020.
- [8] J. Auriol, N. Kazemi, and S.-I. Niculescu. Sensing and computational frameworks for improving drill-string dynamics estimation. *Mechanical Systems and Signal Processing*, 2021 (to appear).
- [9] E. Baum and D. Haussler. What size net gives valid generalization? *Neural computation*, 1(1):151–160, 1989.
- [10] J. F. Brett, A. D. Beckett, C. A. Holt, and D. L. Smith. Uses and Limitations of Drillstring Tension and Torque Models for Monitoring Hole Conditions. *SPE Drilling Engineering*, 4(03):223–229, sep 1989.
- [11] David Cohn, Les Atlas, and Richard Ladner. Improving generalization with active learning. *Machine learning*, 15(2):201–221, 1994.
- [12] I. N. de Almeida Jr, P. D. Antunes, F. O. C. Gonzalez, R. A. Yamachita, A. Nascimento, J. L. Goncalves, et al. A review of telemetry data transmission in unconventional petroleum environments focused on information density and reliability. *Journal of Software Engineering and Applications*, 8(09):455, 2015.
- [13] C. Canudas De Wit, H. Olsson, K. J. Astrom, and P. Lischinsky. A new model for control of systems with friction. *IEEE Transactions on automatic control*, 40(3):419–425, 1995.
- [14] F. Di Meglio, P.-O. Lamare, and U. J. F. Aarsnes. Robust output feedback stabilization of an ODE–PDE–ODE interconnection. *Automatica*, 119:109059, 2020.
- [15] C. Fu, Q.-G. Wang, J. Yu, and C. Lin. Neural network-based finite-time command filtering control for switched nonlinear systems with backlash-like hysteresis. *IEEE Transactions on Neural Networks and Learning Systems*, 2020.
- [16] C. Germa, V. Denoël, and E. Detournay. Multiple mode analysis of the self-excited vibrations of rotary drilling systems. *Journal of Sound and Vibration*, 325(1-2):362–381, aug 2009.
- [17] I. Goodfellow, Y. Bengio, and A. Courville. *Deep learning*. MIT press, 2016.
- [18] G. W. Halsey, A. Kyllingstad, T. V. Aarrestad, and D. Lysne. Drill-string Vibrations: Comparison Between Theory and Experiments on a Full-Scale Research Drilling Rig. In *SPE/IADC Drilling Conference*, number IADC/SPE 14760, pages 311–321. Society of Petroleum Engineers, apr 1986.
- [19] N. Kazemi. Across-domains transferability of deep-red in de-noising and compressive sensing recovery of seismic data. *arXiv preprint arXiv:2007.10250*, 2020.
- [20] N. Kazemi, E. Bongajum, and M. Sacchi. Surface-consistent sparse multichannel blind deconvolution of seismic signals. *IEEE Transactions on geoscience and remote sensing*, 54(6):3200–3207, 2016.
- [21] C. Nwankpa, W. Ijomah, A. Gachagan, and S. Marshall. Activation functions: Comparison of trends in practice and research for deep learning. *arXiv preprint arXiv:1811.03378*, 2018.
- [22] J. Redaud, J. Auriol, and S. I. Niculescu. Output-feedback control of an underactuated network of interconnected hyperbolic pde-ode systems. *System and control letters*, under revision.
- [23] T. Richard, C. Germa, and E. Detournay. Self-excited stick-slip oscillations of drill bits. *Comptes Rendus Mécanique*, 332(8):619–626, aug 2004.
- [24] B. Saldivar, S. Mondié, S.-I. Niculescu, H. Mounier, and I. Boussaada. A control oriented guided tour in oilwell drilling vibration modeling. *Annual Reviews in Control*, 42:100–113, 2016.
- [25] Jian Sun, Kristopher A Inman, and Chao Huang. Physics-guided deep learning for seismic inversion with hybrid training and uncertainty analysis. *Geophysics*, 86(3):1–64, 2021.
- [26] E. Tzeng, J. Hoffman, T. Darrell, and K. Saenko. Simultaneous deep transfer across domains and tasks. In *Proceedings of the IEEE International Conference on Computer Vision*, pages 4068–4076, 2015.
- [27] J. Yosinski, J. Clune, Y. Bengio, and H. Lipson. How transferable are features in deep neural networks? In *Advances in neural information processing systems*, pages 3320–3328, 2014.
- [28] J. Yu, P. Shi, J. Liu, and C. Lin. Neuroadaptive finite-time control for nonlinear mimo systems with input constraint. *IEEE Transactions on Cybernetics*, 2020.
- [29] D.-X. Zhou. Universality of deep convolutional neural networks. *Applied and computational harmonic analysis*, 48(2):787–794, 2020.